Energy confinement scaling for W7-AS high-β plasmas

R. Preuss, A. Dinklage, A. Weller and the W7-AS team

Max-Planck-Institut für Plasmaphysik, EURATOM-Association

Wendelsteinstr. 1, Greifswald, Germany

(Dated:)

Abstract

High-β energy confinement data are subjected to comparisons of scaling invariant, first-principle physical models. The models differ in the inclusion of basic equations indicating the nature of transport. The result for high-β data of the W7-AS stellarator is that global transport is described best with a collisional high-β model, which is different from previous outcomes for low-β data. Model predictive calculations indicate the validation of energy confinement prediction with respect to plasma-β and collisionality ν_*. The finding of different transport behaviors in distinct β regimes is important for the development of fusion energy based on magnetic confinement and for the assessment of different confinement concepts.

PACS numbers: 52.55.Hc, 52.25.Fi, 28.52.-s

Stellarators [1] have proven to be a viable and attractive alternative concept for magnetic confinement due to their potential for steady state operation. Extrapolation capabilities of the plasma performance to next step devices was shown by experimental results from the Large Helical Device (LHD) [2, 3] which could even show enhanced performance with respect to scaling expectations (ISS95 [4]) previously derived without LHD data. For further system studies of reactor size stellarators it is important to investigate variations of operation variables on the global performance for reactor relevant scenarios.

A strategy to explore the scalability of confinement data towards reactor-relevant plasmas is to check the validity of physics models. For stellarators, these model comparisons were motivated by configuration dependencies [2]. E.g. magnetic configurations were shown to have an impact on confinement which could not be rephrased in shaping variables like elongation and triangularity but have to be considered as a configuration characteristics. On the other hand, density and power scalings were recovered in dedicated scans even in high performance operational modes such as the high density H-mode in W7-AS [5].

A particular issue for reactor assessment is the confinement dependence in stellarators on the plasma-β ($\beta = 2\mu_0\langle p/B^2\rangle$), the ratio of the volume averaged kinetic pressure of the plasma and the magnetic field pressure exerted by the toroidal magnetic field. High-β operation is required for economical reactor operation envisaged for a Helias ignition experiment to be at $\beta \lesssim 4.3\%$ [6]. But high-β operation is also to be explored with respect to MHD instabilities and effects on the magnetic configuration, namely the Shafranov shift [7]. Experiments both on W7-AS [8] and LHD [9] demonstrated the accessibility of reactor relevant β values in stellarators not deteriorated by violent MHD [10]. In tokamaks the disagreement between the weak dependence of the energy confinement time on the plasma-β in dedicated scans and the strongly negative dependence derived from scaling laws is unresolved [10]. Therefore, the study of similarities and differences of the β dependence of confinement is one of the key issues for magnetic fusion devices.

Transforming the operation variable dependencies of the latest empirical stellarator scaling laws ISS04 [2], a small degradation of global stellarator confinement with β ($\tau_E^{ISS04} \propto \beta^{-0.17}$) is indicated, which could be due to increased field stochasticity at high β [11, 12]. But data show clustering in device-dependent regions of the collisionality and β. In order to study the leading effects the approach used in this work is based on first principle equations and neglects additional effects due to the dependence of turbulent transport or field

ergodization on β as discussed by Funaba et al. [11]. Since the effect of stochasticity induced transport could be mitigated to a large extent by the control coils in W7-AS, the models employed do not have to cover this as well. For tokamak confinement it was suggested that revealing the scaling with β helps to distinguish between turbulent transport mechanisms, either of electrostatic type showing a small β dependence or of electromagnetic character which are expected to exhibit an unfavorable β scaling [13].

In this paper a tool for testing first principle physical models against global confinement data is employed [14]. For the first time, global confinement data of high-β discharges in the W7-AS stellarator are shown to exhibit a fundamentally different first principle transport behavior. This finding cannot be derived from usual regression analyses or hypothesis tests but requires model comparison techniques. The Bayesian approach employed here is successful since well conditioned data-sets for high-β discharges were available as well as all errors in variables.

The data base examined considers Wendelstein 7-AS confinement data. W7-AS is a partially optimized stellarator in operation from 1988 to 2002 [15]. The high-β data were taken after island divertor installation allowing access to high-β operation. Moreover low-β data before and after divertor installation are included. The operation variables are the mean electron density n, toroidal magnetic field B, absorbed power P and the effective minor radius a. The confinement energy is chosen as scaling target being the measured diamagnetic energy W:

$$W^{theo} \propto n^{\alpha_n} B^{\alpha_B} P^{\alpha_P} a^{\alpha_a} \ . \tag{1}$$

Following Connor and Taylor's (CT) transformation invariance approach [16], constraints on the exponents of the above scaling law can be derived from first principle models by examining the linear transformation behavior of basic model equations. Here, invariance scalings of the Vlasov-, Boltzmann equation and the inclusion of Maxwell equations (encountering β effects by Ampere's law) are considered. Additionally, two fluid models are examined. Both are described by continuity, momentum and energy equation with a choice of ignoring dissipative effects which leads to an either ideal or resistive fluid model according to [17]. The respective constraints on the scaling exponents yield the following scaling law ansatz where the assignment to the specific model is shown in table I.

$$\frac{W^{theo}}{na^4B^2} = c\left(\frac{P}{na^4B^3}\right)^{\xi_1}\left(\frac{a^3B^4}{n}\right)^{\xi_2}\left(\frac{1}{na^2}\right)^{\xi_3} = cf\left(\boldsymbol{\xi}\right) \ . \tag{2}$$

CT-model M_j	ξ_1	ξ_2	ξ_3	N_{dof}	N=96	N=380
Collisionless low-β	x	0	0	1	10^{-24}	10^{-52}
Collisional low-β	x	y	0	2	10^{-19}	10^{-43}
Collisionless high-β	x	0	z	2	10^{-23}	10^{-36}
Collisional high-β	x	y	z	3	1	1
Ideal fluid	x	0	1-x/2	1	10^{-20}	10^{-45}
Resistive fluid	x	y	1-x/2+y	2	10^{-15}	10^{-41}

TABLE I: Connor-Taylor models. N_{dof} is the respective number of variables in the model (dof: degree of freedom). The model probabilities $p(M_j|\boldsymbol{W}^{exp}, \boldsymbol{\sigma}, I)$ are shown in the last two columns for the complete set of all W7-AS high-β data (N=380) and a subset thereof (N=96).

c is a proportionality constant and $f(\boldsymbol{\xi})$ comprises terms with scaling exponents $\boldsymbol{\xi} = (\xi_1, ...)$. Note that the number of multiplicative terms – or *CT variables* – (i.e. scaling exponents) N_{dof} varies between one and three, e.g. in the simplest case of the collisionless low-β model there is only one scaling exponent $\xi_1 = x$ left. Since for the first four rows in table I the models with more degrees of freedom N_{dof} include the simpler models it is to be expected that more complex models fit the data better in a least square (χ^2) sense. But the method of Bayesian model comparison overcomes the drawback of over-fitting by *Occam's razor*, i.e. the reduction of χ^2 is encountered by the burden of an enlarged parameter space, which size is accumulating with the number of fitting parameters [18]. The larger this parameter space gets, the more difficult it becomes to justify further introduced parameters by the gain in description.

A successful application of this approach led to the results in [14], i.e. that the low-β data of W7-AS are described by the collisional low-β CT-model. Moreover it was possible to overcome the shortcoming of common scaling laws to describe the saturation of confinement, e.g., with n. This follows from exploiting the invariance principle one step further and to scale not over a single term but over a sum of scaling terms $f(\boldsymbol{\xi}_k)$ with expansion coefficients c_k (which was already stated in the original formulation of Ref. [16]):

$$W^{theo} = na^4B^2 \sum_{k=1}^{E} c_k f\left(\boldsymbol{\xi}_k\right) \ . \tag{3}$$

Since a sum is a linear operation the transformation properties of Eq. (2) are conserved.

The optimum expansion order E is an outcome of the probabilistic approach applied here.

Probabilistic model comparison employs conditional probabilities $p(M|\boldsymbol{W}^{exp}, \boldsymbol{\sigma}, I)$ to assess model M given confinement data $\boldsymbol{W}^{exp}$ and their uncertainties $\boldsymbol{\sigma}$ under the context information I summarizing the choice of models and assumptions. The model comparison is the evaluation of the so-called odds ratio which is the factor of the *posterior* probabilities of two models M_k and M_j to be compared on the basis of the same data [18].

$$\frac{p(M_j|\boldsymbol{W}^{exp}, \boldsymbol{\sigma}, I)}{p(M_k|\boldsymbol{W}^{exp}, \boldsymbol{\sigma}, I)} = \frac{p(M_j|I)}{p(M_k|I)} \frac{p(\boldsymbol{W}^{exp}|M_j, \boldsymbol{\sigma}, I)}{p(\boldsymbol{W}^{exp}|M_k, \boldsymbol{\sigma}, I)} \ . \tag{4}$$

The prior odds (first ratio on the r.h.s.) is set constant, i.e. no model is preferred *a priori*. The second ratio, the so-called Bayes factor, is obtained by summing over all expansion orders of Eq. (3)

$$p(\boldsymbol{W}^{exp}|M_j, \boldsymbol{\sigma}, I) = \sum_E p(E|M_j, I) p(\boldsymbol{W}^{exp}|E, M_j, \boldsymbol{\sigma}, I) \ , \tag{5}$$

where $p(E|M_j, I)$ is set constant again because *a priori* no expansion order is favored. To get the marginal likelihood $p(\boldsymbol{W}^{exp}|E, M_j, \boldsymbol{\sigma}, I)$ we proceed as follows:

The uncertainties $\boldsymbol{\sigma}$ of the energy content contain the direct distributions from the diamagnetic measurement as well as the errors in the operation variables. In order to test for deviations of the experimental errors a factor ω is introduced which can be regarded to describe the statistical scatter between data and model. It is self-consistently calculated by the analysis. For N data this leads to the following likelihood function

$$p(\boldsymbol{W}^{exp}|\omega, \boldsymbol{c}, \boldsymbol{\xi}, E, M_j, \boldsymbol{\sigma}, I) = \left(\frac{\omega}{2\pi}\right)^{\frac{N}{2}} \frac{1}{\prod_i^N \sigma_i}$$
$$\cdot \exp\left\{ -\omega \sum_{i=1}^{N} \left[W_i^{exp} - \sum_k^E c_k f_i(\boldsymbol{\xi}_k) \right]^2 / 2\sigma_i^2 \right\} \ . \tag{6}$$

The marginal $p(\boldsymbol{W}^{exp}|E, M_j, \boldsymbol{\sigma}, I)$ is obtained by integrating Eq. (6) and respective priors over $\boldsymbol{c}$, ω and the scaling exponents $\boldsymbol{\xi}$. While for $\boldsymbol{c}$ and ω the integral has an analytical solution one is left for the integration over $\boldsymbol{\xi}$ with Markov chain Monte Carlo techniques employing the thermodynamic integration scheme [19]. Note that these integrations finally result in the model probabilities of Eq. (4) and not in a best set of fitting parameters for a scaling law.

Fig. 1 shows β and collisionality ν_*= $16R_0\nu_{th}/3\pi t v_{th}$ (normalized to the onset of the

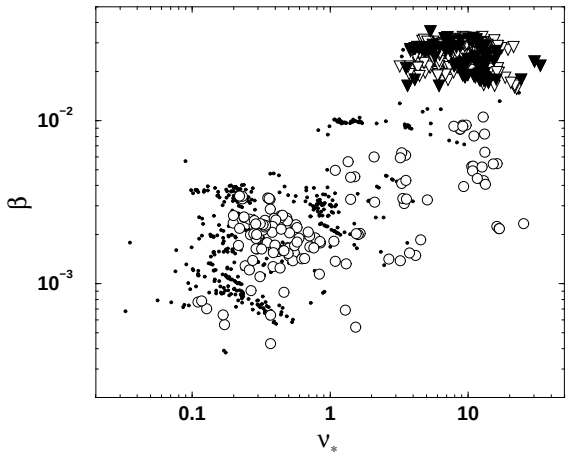

FIG. 1: Examined W7-AS confinement data as a function of β and collisionality ν_*($\circ$ low-β, $\triangledown$ high-β, $\blacktriangledown$ high-β subset ($0.45 < \iota < 0.49$), $\cdot$ further W7-AS data in ISCDB).

Pfirsch-Schlüter regime; ν_{th} and v_{th} consist of volume averaged plasma parameters) values of available confinement data documented in the International Stellarator Confinement Data Base (ISCDB) [20]. From those three subsets were examined.

First, N=153 low-β data were taken at full (B=2.5T) and half field with $\beta < 1\%$ for reference. The data are restricted to a small window of the rotational transform at $\iota = 0.33 \ldots 0.35$ since otherwise the plasma energy W varies up to a factor of two as a function of the rotational transform ι [21]. The value of the rotational transform is taken at 2/3 of the effective plasma radius and stems from finite-β equilibrium calculations. Second, the high-β data were assembled from high-power neutral-beam injection discharges at reduced magnetic field $|B| < 1.5$T with residual plasma currents less than 500A. Compared to the low-β case, the dependence of the energy content on ι is quite smooth for high-β plasmas [8]. Therefore all shots were included in the high-β data set (triangles in Fig. 1), apart from nine shots which establish a power scan used for validation (see below). Only stationary phases of the discharges were considered. Finally a total of 389 shots met the criteria and entered the high-β W7-AS ISCDB subset. Third, a subgroup of the high-β data was chosen for $0.45 < \iota < 0.49$ to test the robustness of model comparison and to check dependency on ι. Here, the energy content for these ι values and B=1.25T passes through a broad maximum with variation of less than 10% [8]. This led to a second high-β set with N=96 entries (filled triangles in Fig. 1).

The result of the model comparison for the two high-β sets is stated in the rightmost

column of table I. The figures comprise a sum over all relevant expansion orders in Eq. (5). It turns out that for the most likely model the most probable expansion order is three. Both high-β W7-AS data sets are best described by the collisional high-β model (CHB). This is different to the previous result for the low-β subset where the collisional low-β model was the most probable one. Therefore the present paper proves the capability of Bayesian model comparison to identify differences in the β-behavior from invariance considerations. The finding of a collisional model corresponds to the expectations since even for the low-β data set the plasma is influenced by relative high collisionalities of the ions which are still in the plateau regime.

Bayesian model comparison allows to assign the probabilities among a given set of models rather than the acceptance of a single null-hypothesis. The impact of additional models is easily examined. This was already done in the present analysis where a fluid description was found to describe the data much worse than a collisional kinetic model. Introducing so-called non-neutral models, which encounter for effects on the Debye length scale, generates in Eq. (2) a new term B^2/n with respective scaling exponent ξ_4. The model comparison leads to a significant probability for the non-neutral collisionless high-β model (NHB, terms with scaling exponents ξ_1, ξ_3 and ξ_4). However, the most probable CHB model and the most probable non-neutral model NHB deviate only by exchanging the "collisionality"-term a^3B^4/n with the "non-neutrality"-term B^2/n. With an effective minor radius hardly varying around 15cm and a strong clustering of the magnetic field at 1.2T the data base is too badly conditioned to discriminate between both models. This is corroborated by a high linear correlation coefficient for the responsible two terms. Since the considered high-β plasmas of W7-AS are of high density and low temperature collisions among the plasma particles play a major role. Therefore it is not to be expected that violations of charge neutrality exist and non-neutral models can be excluded by physics considerations. But the above exercise indicates the limits to identify the correct model: Only models can be distinguished for which the data set offers sufficient discrimination in the respective CT-variables. This is the case for the terms discriminating low- and high-β or collisional and collisionless models. In order to access non-neutral models a better coverage of the minor radius and toroidal magnetic field space is required.

Once the most probable model is identified, it is straightforward to calculate expectation values for distinct operation variables. This is shown for density and power scans in Fig.

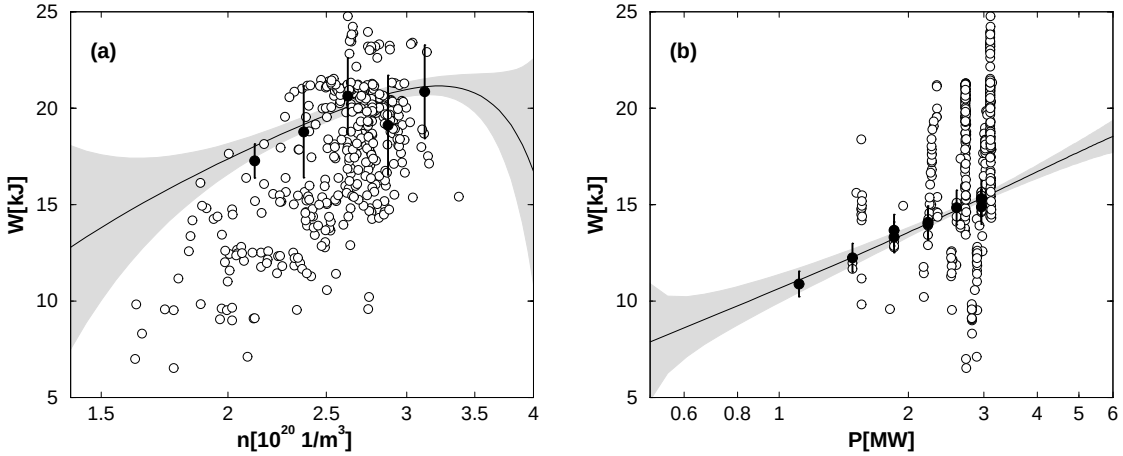

FIG. 2: Energy content of the high-β data (open circles) as function of (a) density and (b) absorbed power. Solid line (with grey shaded area): prediction (and its uncertainty) of the collisional high-β model for (a) density scan ($P = 3.1$MW, $B = 1.18$T, $a = 0.152$m) and (b) power scan ($n = 2.4 \cdot 10^{20}\mathrm{m}^{-3}$, $B = 0.95$T, $a = 0.154$m). Experimental data for these settings are the full circles with error bars.

2. Since all high-β data vary in all settings of the operation variables, the projections of W values on the density n and the heating power P, respectively, appear as scattered plots. In order to validate the scaling results it is useful and instructive to compare predictions from the present analysis with experimental single variable scans. Fig. 2 shows such a comparison. The uncertainty range (grey shaded area) defines where the result may be trusted. It is smallest where the support from the data is largest. Outside this range the uncertainty of the prediction increases rapidly for the density, but still shows a saturation effect (as was the case in the low-β dataset). The power scan stays close to a log-linear behavior with a scaling exponent of about $\alpha_P \approx 0.4$. Only a few experiments were performed with varying power but a stiff setting of the rest of the operation variables. The results of these experiments are not contained in the high-β data base under consideration and therefore serve as an independent check of the prediction (see Fig. 2b). The agreement is excellent. For the density no dedicated experimental scan exists, but a validation of the model prediction can be performed nonetheless. Thereto all energy contents were gathered which are close to a fictitious density scan for $P = 3.1$MW, $B = 1.18$T, $a = 0.152$m. Within equidistant ranges on the density axis mean values of those data were formed. Five such averages (full circles in Fig. 2a) are shown with error-bars originating from the spread of the data (therefore they

differ in size from the actual experimental error-bars of the full circles in Fig. 2b). The prediction coincides very well with these points.

A scatter plot (not shown) of the experimentally obtained plasma-β versus predictions from the collisional high-β model gives a diagonal distribution as expected, however, a factor of two broader than the standard deviations of the values suggest. This indicates the presence of additional physical phenomena in the plasma (e.g. wall condition, impurity content or heating efficiency) not covered by the scaling law approach within the CHB model. Still, the scatter is smallest compared with the other CT-models.

As empirically suggested in the previous ISS04 study, these results demonstrate different first-principle physics exhibited in global confinement data in W7-AS. High-β data from W7-AS need to include electromagnetic effects differently to low-β data. Furthermore, the predictive model indicates a saturation of confined energy with density at highest densities, whereas power scaling behaves log-linearly, however with a slightly smaller scaling exponent than previously revealed in global scaling laws.

For scaling towards reactor scenarios, the present result suggests a strategy different to usual scaling approaches: Rather sampling data from a wide range of operation variables, experiments matching partially reactor target variables can be analyzed to yield information on first-principle mechanisms. Following the general idea of scaling invariances, variables should be chosen in figures of dimensionless quantities such as the plasma-β. The findings then can be used to supplement transport simulations of reactor scenarios. For stellarators, the next step should be extended to long-mean-free path physics which is reachable in LHD and will be provided in W7-X.

We appreciate discussions with C.D. Beidler, R. Brakel, V. Dose, R. Fischer, J. Geiger, S. Gori, J.H.H. Harris, A. Kus, H. Maaßberg, U. Stroth, U. von Toussaint, F. Wagner and H. Yamada.

This work was partly conducted within SFB TR 24, project B8-A.

---

1 A. Boozer, Phys. Plasmas **5**, 1647 (1998).

2 H. Yamada et al., Nucl. Fusion **45**, 1684 (2005).

3 S. Murakami et al., Fusion Sci. Technol. **51**, 112 (2007).

4 U. Stroth et al., Nucl. Fusion **36**, 1063 (1996).

5 A. Dinklage et al., Fusion Sci. Technol. **51**, 1 (2007).

6 H. Wobig et al., Nucl. Fusion **43**, 889 (2003).

7 V. Shafranov, J. of Nucl. Energy C **5**, 251 (1963).

8 A. Weller et al., Plasma Phys. Control. Fusion **45**, A285 (2003).

9 S. Sakakibara et al., Fusion Sci. Technol. **50**, 177 (2006).

10 D. McDonald et al., Plasma Phys. Control. Fusion **46**, A215 (2004).

11 H. Funaba et al., Fusion Sci. Technol. **51**, 129 (2007).

12 A. Weller et al., Fusion Sci. Technol. **50**, 158 (2006).

13 C. Petty et al., Phys. Plasmas **11**, 2514 (2004).

14 V. Dose, R. Preuss, and W. von der Linden, Phys. Rev. Lett. **81**, 3407 (1998).

15 F. Wagner et al., Phys. Plasmas **12**, 072509 (2005).

16 J. W. Connor and J. B. Taylor, Nucl. Fusion **17**, 1047 (1977).

17 J. W. Connor, Plasma Phys. Control. Fusion **30**, 619 (1988).

18 E. T. Jaynes, *The Logic of Science* (Oxford University Press, Oxford, 2005).

19 W. von der Linden, R. Preuss, and V. Dose, in *Maximum Entropy and Bayesian Methods*, edited by W. von der Linden et al. (Kluwer Academic, Dordrecht, 1999), p. 319.

20 URL of ISCDB: http://www.ipp.mpg.de/ISS and http://iscdb.nifs.ac.jp/.

21 R. Brakel et al., Nucl. Fusion **42**, 903 (2002).